Soil Dynamics and Earthquake Engineering 89 (2016) 208–218

Contents lists available at ScienceDirect

Soil Dynamics and Earthquake Engineering

journal homepage: www.elsevier.com/locate/soildyn

The effect of grain size on G_{max} of a demolished structural concrete: A study through energy dispersive spectroscopy analysis and dynamic element testing

H. He, K. Senetakis *

University of New South Wales, Sydney, Australia

ARTICLE INFO

Article history:
Received 5 January 2016
Received in revised form
1 May 2016
Accepted 8 August 2016

Keywords:
Resonant column
Bender elements
Elastic shear-modulus
Sand
Recycled concrete aggregate
Particle shape
Mean grain size
State parameter
Scanning electron microscope
Energy dispersive spectroscopy

ABSTRACT

Recycled concrete aggregate (RCA) composed of demolition-crushed structural concrete is a promising material in geotechnical engineering applications, for example, as a backfill in retaining walls or as an embankment fill and pavement construction material. Due to the presence of cement mortar component, RCA has a lower unit weight than that of typical soils, thus its use may be considered beneficial in engineering infrastructures with a demand in the reduction of settlements or lateral earth pressures. In this study, a set of torsional resonant column and bender element tests were carried out on uniform fractions of a recycled concrete aggregate with origin from New South Wales, Australia, with varying the mean grain size. The created in the laboratory samples, were prepared in a dry state and tested under isotropic conditions of the confinement varying the effective confining stress from 25 to 800 kPa in a resonant column and in a triaxial apparatus with embedded piezo-element inserts with a particular focus on the elastic stiffness G_{max}. The results showed that the sensitivity of G_{max} to pressure increased with decreasing mean grain size. This observed trend was attributed, partly, to the higher cement mortar component for fractions with a smaller grain size. The different composition of the fractions was verified through Scanning Electron Microscope - Energy Dispersive Spectroscopy (SEM-EDS) analysis in particular quantifying the ratio of Silicon over Calcium contents. The performance of expressions proposed in the literature for the prediction of G_{max} of sands and gravels, was rigorously evaluated by means of measured against predicted elastic stiffness for all the fractions as well as by means of the state parameter for a particular RCA fraction.

1. Introduction

The prediction of ground deformations and the response of geo-structures subjected to static or dynamic load patterns, require the knowledge of soil shear modulus (G) and its dependency to the confining stress and shear strain levels [18]. At very small strains, in general less than 10^{-3}%, G corresponds to its maximum value (denoted as G_{max}) and expresses an elastic property. For any geo-material, G_{max} is a constant-state property [9,28] and it can be described by two independent quantities: the current confining pressure (p′) and the current void ratio (e). Accurate measurements of G_{max} in the laboratory, require the application of dynamic test methods. The resonant column is one of the popular and standardized methods for this purpose [18,27,3]. Recently, the use of piezo-element testing has received great attention and applications in soil mechanics and dynamics research due to the easy implementation of the piezo-element inserts in any triaxial-type device and the straightforward determination of the shear wave velocity from the distance between the inserts and the determination of the time arrival of the waves [15,21,35].

In the past decades, the elastic shear-modulus of geo-materials has been examined extensively. With respect to granular geo-materials subjected to isotropic or closely isotropic conditions of the confining pressure, the basic concluding remarks from the literature are that G_{max} is affected, apart from the important roles of (p′) and (e), by the coefficient of uniformity [11,19,24,40,30,32], the shape of particles [13,14,25] and the type of the soil by means of mineral components and grain morphology [30–33]. A recent research work by Yang and Gu [38] showed that the grain size, which is commonly expressed through the mean grain size (d_{50}), does not affect significantly the elastic shear-modulus of sand-size soils, which observation is in agreement with the previous works by Menq [24], Wichtmann and Triantafyllidis [40] and Senetakis et al. [30]. The sensitivity of G_{max} to pressure has been linked to the behavior at the grain scale, the nature of the grain-to-grain contact response and the magnitude and distribution of the

* Corresponding author.
E-mail address: k.senetakis@unsw.edu.au (K. Senetakis).

http://dx.doi.org/10.1016/j.soildyn.2016.08.011
0267-7261/

contact forces within a granular assembly of grains [28,29,9], which in turn are affected by the previously mentioned characteristics, for example, the grain size distribution or the shape of the grains.

Referring to granular geo-materials, most published research works in the literature have focused on natural soils or crushed rock of a single mineral type or, soils with one dominant mineral. In the present study, an effort was attempted to study in the laboratory the elastic shear-modulus of an engineered sand composed of recycled concrete aggregate (RCA) which is the product of demolition-crushed structural concrete. Due to the presence of aggregate and cement mortar as the dominant components, the behavior of this material may be more complex since the exact percentages of the variable components may not be known always. In particular, the content of cement decreases with increases the size of the RCA fraction [36]. Apart of its academic interest as a complex granular material with a low unit weight and the presence of two dominant solid components, i.e. aggregate and cement mortar, as well as the challenges to study in the laboratory the dynamic properties of RCA, it is a material that may find many applications in civil engineering projects and pavement geotechnics [1,12,2,26,34,36,37,8]. This is because of the recent pressing need to utilize recycled and demolition aggregates in beneficial ways. Recycled concrete aggregate composed of demolished-crushed structural concrete is one of these waste materials that the research community has recently focused on due to its interesting properties and promising performance from both structural and geotechnical engineering perspectives.

Previous research works have focused, primarily, on the re-use of RCA for the production of new structural concrete, but recently many studies have shown promising properties and potential applications of RCA in geotechnical projects, for example in pavement geotechnics and earth retaining support structures. In this regard, the present work focused on the elastic shear modulus (G_{max}) of a recycled concrete aggregate with origin from New South Wales, Australia, and in particular on the sensitivity of G_{max} to pressure (p′) and mean grain size (d_{50}). For this purpose, samples with varying d_{50} were prepared in the laboratory and tested in a resonant column in the range of very small shear strains with $\gamma < 10^{-3}\%$. The performance of literature expressions for the prediction of G_{max} of sands and gravels was evaluated by means of predicted against measured shear modulus, denoted as $G_{max,p}$ and $G_{max,m}$, respectively, for all the RCA fractions as well as by means of the ratio $G_{max,m}/G_{max,p}$ against the state parameter for a particular RCA fraction. In order to assess the changes of cement mortar and aggregate components for the different fractions, Scanning Electron Microscope - Energy Dispersive Spectroscopy (SEM-EDS) analysis was carried out on different fractions as well as on a sample composed of pure cement and the ratio of silicon over the calcium contents was quantified.

2. Materials and methods

2.1. Parent demolition material and uniform fractions used in the study

A recycled concrete aggregate composed of demolished-crushed structural concrete from New South Wales, Australia, was used in the study. The parent aggregate is a well-graded material composed of aggregate and cement mortar as the dominant components, with the presence of silt-size grains and brick. The parent aggregate was prepared through a set of sieves and five uniform fractions were separated and used in the study, denoted as RCA02 (fraction 0.15–0.30 mm), RCA03 (fraction 0.30–0.60 mm), RCA04 (fraction 0.60–1.18 mm), RCA05 (fraction 1.18–2.36 mm) and RCA06 (fraction 2.36–4.75 mm). The grading curves of the five fractions are illustrated in Fig. 1. The grain size characteristics (mean grain size, d_{50}, and coefficient of uniformity, C_u) and the specific gravity of solids (G_s) are summarized in Table 1. G_s was determined adopting the ASTM D854-02 specification [4]. It was found that G_s varied slightly with the RCA fraction but the values did not monotonically increase or decrease with d_{50}. An image for the fraction RCA05 is given in Fig. 2.

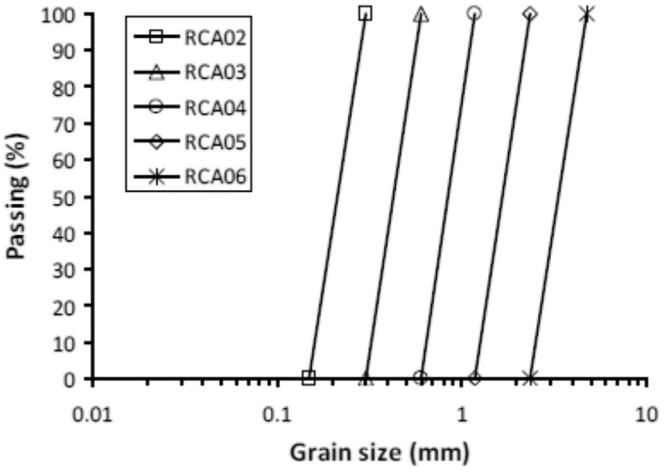

Fig. 1. Grading curves of recycled concrete aggregate (RCA) fractions used in the study and typical image taken from an optical microscope of an individual grain.

Table 1
Recycled concrete aggregate (RCA) fractions used in the study.

Code of sample	RCA02	RCA03	RCA04	RCA05	RCA06
Fraction (mm)	0.15–0.30	0.30–0.60	0.60–1.18	1.18–2.36	2.35–4.75
Specific gravity G_s	2.62	2.48	2.47	2.47	2.59
Mean grain size d_{50} (mm)	0.21	0.42	0.84	1.67	3.35
Coefficient of uniformity C_u	1.35	1.62	1.35	1.37	1.42
Sphericity R (mean)	0.71	0.59	0.71	0.67	0.56
Sphericity standard deviation	0.16	0.17	0.15	0.21	0.19
Roundness (mean)	0.49	0.29	0.29	0.31	0.23
Roundness standard deviation	0.17	0.13	0.13	0.16	0.11
Regularity ρ	0.60	0.44	0.50	0.49	0.40
Regularity standard deviation	0.13	0.11	0.13	0.15	0.12

Fig. 2. Typical image of recycled concrete aggregate fraction 1.18–2.36 mm.

2.2. Scanning electron microscope - energy dispersive spectroscopy analysis

Due to the presence of cement mortar and aggregate components with varying percentages for the variable fractions, it is expected that the composition of the RCA may play an important role on the dynamic properties of this complex material, in particular on the sensitivity of stiffness to pressure. Works published in the literature (summarized by [36]) have indicated that the cement mortar component decreases with increasing the grain size of the RCA. This is reasonable to expect since the parent cement is composed of finer size grains and the demolition process, which results in a crushed material, will produce a binary mixture with higher percentage of cement for finer size of the RCA. Typically, for pure cement, the content of silicon is very similar to the content of calcium. For the recycled concrete aggregate, the silicon content is the dominant (e.g. [6]) but there is presence of variable minerals. A strong indication of the change of cement mortar and aggregate components is given from the ratio of silicon over the calcium contents (Si/Ca), with greater values of this ratio indicating a lower percentage of cement mortar.

A straightforward method to estimate the ratio (Si/Ca) is the use of Scanning Electron Microscope - Energy Dispersive Spectroscopy (SEM-EDS) Analysis [22]. In the present study, SEM-EDS analysis was conducted for fractions RCA02, RCA03, RCA05 and RCA06 at the Mark Wainwright Analytical Center of UNSW. Typical SEM images of two RCA fractions are given in Fig. 3. Typical plot of SEM-EDS analysis by means of intensity (counts) again the energy is given in Fig. 4 indicating the peaks of Silicon and Calcium. This set of experiments indicated a clear increase of the ratio (Si/Ca) for greater grain size of the RCA fractions. A sample composed of dominantly cement mortar was also tested through SEM-EDS analysis which indicated similar contents of silicon and calcium. These results, summarized in Fig. 5, indicate a tendency of greater aggregate and lower cement mortar components with increasing the size of the RCA fraction.

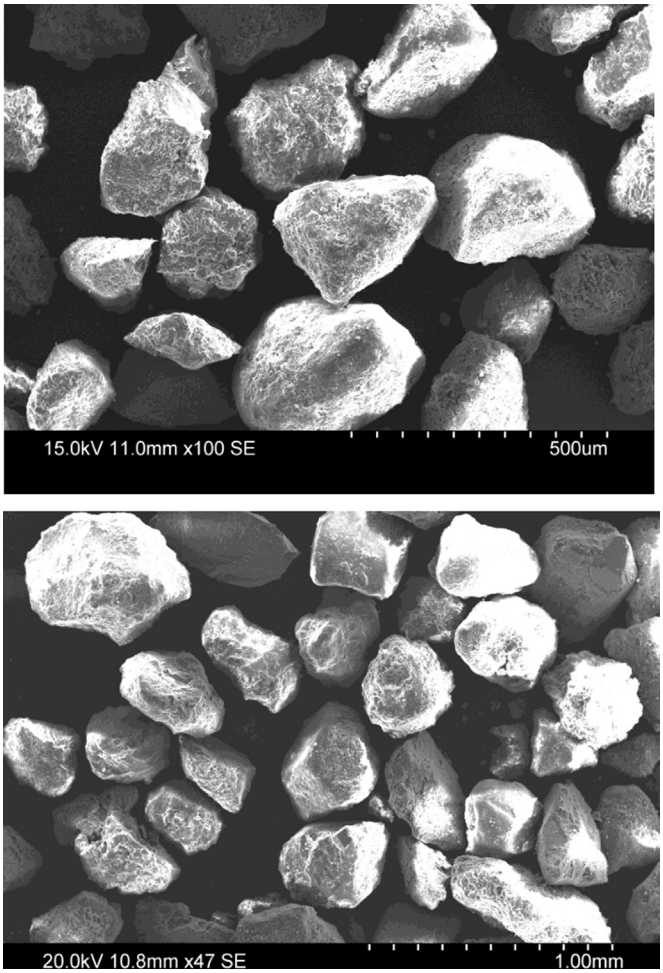

Fig. 3. Scanning Electron Microscope (SEM) images of fractions RCA02 (top image) and RCA03 (bottom image).

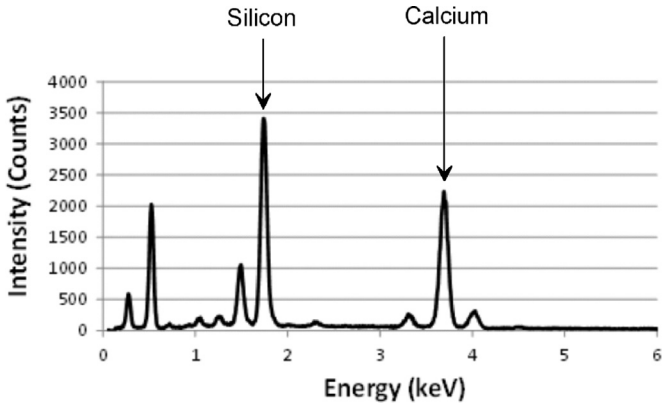

Fig. 4. Typical plot of Scanning Electron Microscope - Energy Dispersive Spectroscopy (SEM-EDS) analysis.

2.3. Quantification of particle shape descriptors and their role on G_{max} of granular soils

In the study, the shape of particles of the RCA fractions was quantified by examining a representative number of grains through an optical microscope and using an empirical chart proposed by Krumbein and Sloss [23], which chart is given in Fig. 6 (modified by the authors). Additionally, the quantification of particle shape was supported by visual observation of the grains through the SEM analysis, as for example the images of Fig. 3. In particular, a set of grains from each fraction were randomly chosen and three shape descriptors were quantified; the sphericity (S), the roundness (R) and the regularity (ρ). The regularity was introduced by Cho et al. [13] in order to capture, quantitatively, the effects of both roundness and sphericity in the mechanical behavior of granular materials. The arithmetic value of (ρ) is defined

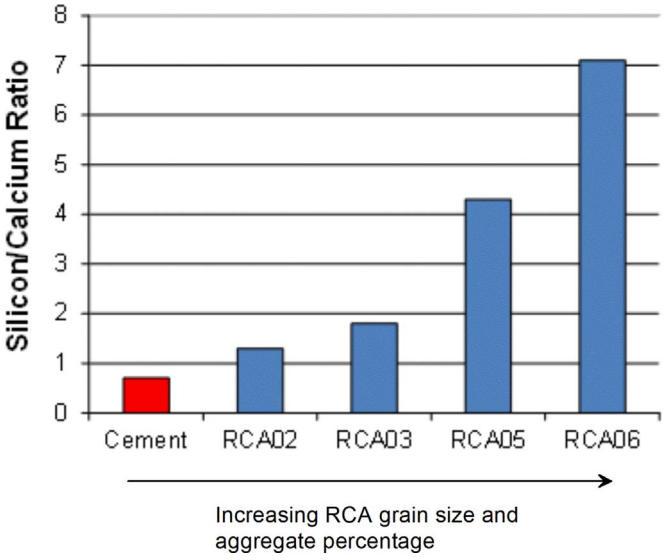

Fig. 5. SEM-EDS results: ratio of silicon over calcium contents for the variable RCA fractions.

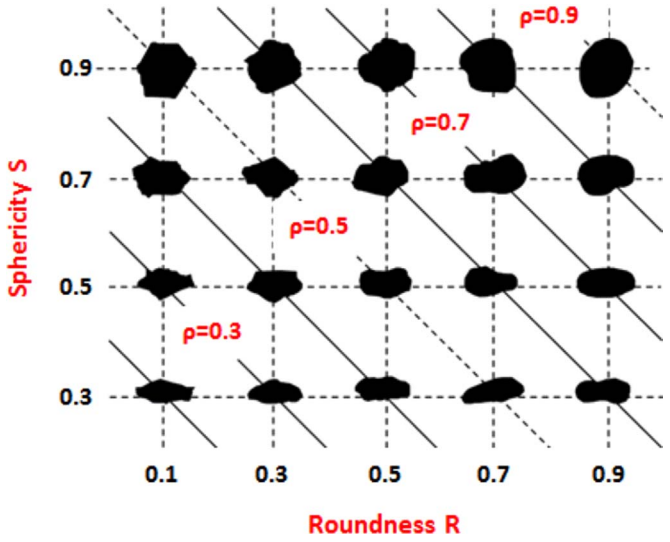

Fig. 6. The empirical chart used in the study for the particle shape quantification (after [23]).

from Eq. (1).

$$\rho = \frac{S + R}{2} \tag{1}$$

Based on the total number of grains examined from each fraction, the mean and standard deviation values of the shape descriptors (S), (R) and (ρ) were determined. These values are summarized in Table 1. In Fig. 7, the variation of the shape descriptors against the mean grain size for the five RCA fractions is illustrated. It was found that d_{50} had a small effect on the shape descriptors, but the observed trend was a slight decrease of the regularity with d_{50}, thus the grains became slightly more irregular in shape for the coarser fractions.

G_{max} of granular soils is fully defined by two independent quantities; the void ratio (e) and the mean effective confining pressure (p′). The general expression for the elastic stiffness of granular soils is given in Eq. (2), where A_G and n_G express elastic constants, p_A is the atmospheric pressure, which pressure is used for normalization purposes, and F(e) is the void ratio function.

$$G_{max} = A_G \times F(e) \times \left(\frac{p'}{p_A}\right)^{n_G} \tag{2}$$

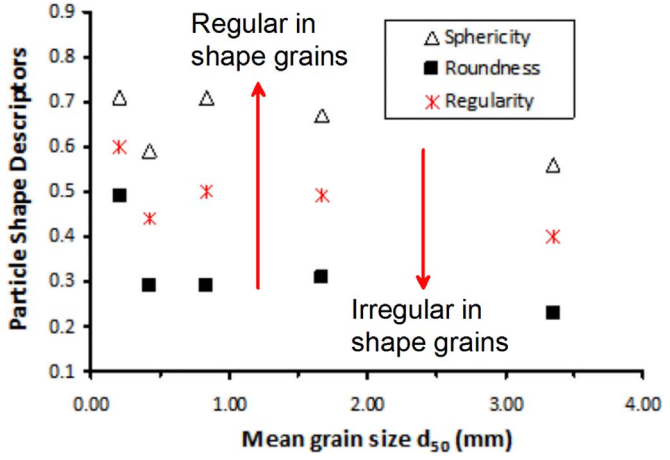

Fig. 7. The variation of particle shape descriptors with the mean grain size for the recycled concrete aggregate fractions.

Many laboratory research studies have demonstrated the important effect of the coefficient of uniformity (C_u) on the elastic constants of Eq. (2). Cho et al. [13] and Payan et al. [25] quantified the effect of the shape descriptors on the elastic constants A_G and n_G. Both studies found that A_G decreases, whereas n_G increases, with a decrease of the magnitude of the shape descriptor (ρ). Thus, the absolute value of G_{max} at a given (p′) and a given (e) and the sensitivity of G_{max} to the confining pressure are significantly affected by the grain shape. However, at least for sand-size granular materials, previous research works have not found a clear effect of d_{50} on G_{max} (e.g. [40,30,38]).

RCA is a material with two dominant components: aggregate and cement mortar components, and in particular the cement mortar component increases for finer fractions as also demonstrated from the SEM-EDS analysis of the study (Fig. 5). Therefore, it may be expected some effect of d_{50} on the elastic stiffness of the recycled concrete aggregate due to the different composition of the variable fractions. In the present study, the shape of the RCA particles was quantified in order to decouple the possible effects, if any, of the particle shape and the mean grain size on the elastic stiffness (G_{max}) of the RCA.

2.4. Equipment used

G_{max} of the RCA fractions was examined on dry samples in a resonant column apparatus of fixed-free ends as well as through bender element tests using piezo-element inserts embedded in a triaxial apparatus. The laboratory devices used (resonant column and triaxial with embedded piezo-elements) are computer-controlled systems supplied by GDS Instruments, UK, and thy can accommodate samples of about 50 mm in diameter and 100 mm in length. For the resonant column tests and the analysis of the results, the ASTM D4015-92 specification was used. For the bender element tests, the first-time arrival method was used for the estimation of the shear wave velocity (V_s) applying an input pulse of sinusoidal type of 10 kHz. Based on the shear wave velocity and the density (ρ) of the sample, the small-strain shear modulus was computed based on the well-known formula of Eq. (3).

$$G_{max} = \rho \times V_s^2 \tag{3}$$

Details of the interpretation of the bender elements signal adopted in the study may be found in He and Senetakis [17]. Based on their analysis, He and Senetakis found minimum effect of the excitation frequency on V_s as well as a satisfactory agreement between bender element tests and torsional resonant column tests with respect to the resultant G_{max}.

2.5. Sample preparation and dynamic testing program

From each fraction, three to five samples were prepared in a dry state in the resonant column or the triaxial apparatus using a split plastic mold of appropriate dimensions. The samples were prepared at variable initial densities. Medium dense to very dense samples were compacted in layers and for each layer vibration was applied through a plastic thin rod with rounded edges, while for medium dense to loose samples, the air-pluviation method was used. In total, eighteen samples (summarized in Table 2) were prepared and tested in a dry state under isotropic conditions of the confining pressure (p′), varying from 25 or 50 to 800 kPa. Note the very low unit weight and relatively high void ratio of the samples as shown in Table 2. Vacuum of 5 kPa was applied to the sample before the set-up of the system. For each sample, low-amplitude torsional resonant column tests in the resonant column or bender element tests in the triaxial apparatus were conducted at variable confining pressures (p′).

Table 2
Dynamic testing program on dry samples.

No.	Specimen code	Fraction (mm)	Dynamic testing method	Preparation method	e_o	γ_{do} (kN/m^3)
(1)	(2)	(3)	(4)	(5)	(6)	(7)
1	RCA02–1	0.15–0.30	Resonant column	Air-pluviation	1.384	10.78
2	RCA02–2	0.15–0.30	Resonant column	Compaction	1.274	11.30
3	RCA02–3	0.15–0.30	Resonant column	Air-pluviation	1.368	10.85
4	RCA02–4	0.15–0.30	Bender elements	Compaction	1.190	11.74
5	RCA02–5	0.15–0.30	Bender elements	Compaction	1.347	10.95
6	RCA03–1	0.30–0.60	Resonant column	Compaction	1.056	11.83
7	RCA03–2	0.30–0.60	Resonant column	Compaction	0.934	12.58
8	RCA03–3	0.30–0.60	Bender elements	Compaction	1.054	11.84
9	RCA04–1	0.60–1.18	Resonant column	Air-pluviation	1.264	10.70
10	RCA04–2	0.60–1.18	Resonant column	Compaction	1.175	11.14
11	RCA04–3	0.60–1.18	Resonant column	Compaction	1.136	11.34
12	RCA04–4	0.60–1.18	Resonant column	Compaction	1.171	11.16
13	RCA05–1	1.18–2.36	Resonant column	Compaction	1.233	10.85
14	RCA05–2	1.18–2.36	Resonant column	Compaction	1.200	11.01
15	RCA05–3	1.18–2.36	Resonant column	Compaction	1.248	10.78
16	RCA06–1	2.36–4.75	Resonant column	Air-pluviation	1.255	11.27
17	RCA06–2	2.36–4.75	Resonant column	Compaction	1.214	11.48
18	RCA06–3	2.36–4.75	Bender elements	Compaction	1.171	11.70

Note: e_o and γ_{do} denote initial void ratio and unit weight while the samples were supported by a vacuum of 5 kPa.

The present study focused on the effect of d_{50} on the elastic shear modulus (G_{max}) of the RCA fractions. He and Senetakis [17] studied two fractions (RCA04 and RCA05), in particular investigating through piezo-element (bender/extender element) tests, the S-wave and P-wave velocities and the small-strain Poisson ratio, as well as, through high-amplitude resonant column tests, the small-to-medium strain modulus degradation and damping increase. A discussion on comparisons between resonant column and piezo-element tests is also presented by He and Senetakis [17]. In that study, G_{max} of the RCA04 and RCA05 fractions was compared with the predicted values from two models proposed by Senetakis et al. [30]; one G_{max} model derived on the basis of rounded-river sand and one G_{max} model derived on the basis of crushed rock of irregular-shaped grains. In the present study, the evaluation of variable models from the literature is thoroughly examined for all the RCA fractions by means of estimated over measured G_{max} as well as, for the fraction RCA04, by means of the state parameter concept as discussed by Payan et al. [25].

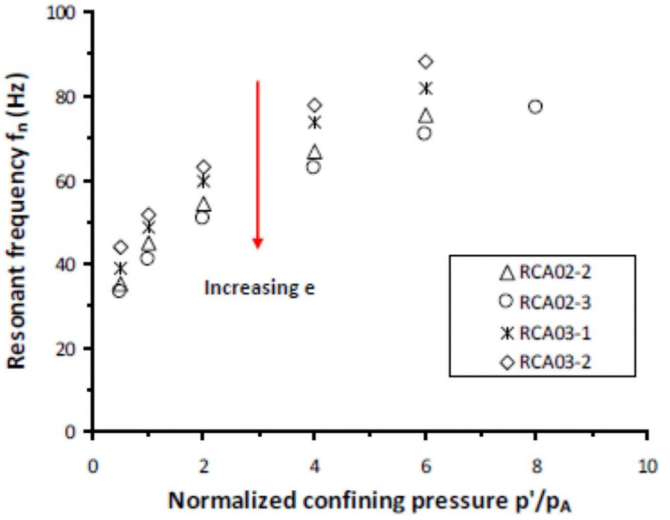

Fig. 8. Typical plots of the resonant frequency against the normalized confining pressure for the fraction RCA02 (0.15–0.30 mm) and the fraction RCA03 (0.30–0.60 mm).

3. Results and discussion

3.1. Representative test results

Typical plots of resonant frequency (f_n) against the confining pressure (p'/p_A), normalized with respect to the atmospheric pressure (p_A), and G_{max} against (p'/p_A) are given in Figs. 8 and 9, respectively, for fractions RCA02 and RCA03. f_n depends on the type of the geo-material in consideration, its density as well as the size of the resonant column specimen [33]. For the particular fractions and size of specimens (50 mm in diameter and 100 mm in length), f_n ranged from about 30–45 Hz at $p'=50$ kPa, to about 70–90 Hz at $p'=600$ kPa. For a given level of (p'), f_n decreased for samples with a greater void ratio, as illustrated in Fig. 8. Similarly, G_{max} increased with (p') and decreased for samples with a greater void ratio (Fig. 9). In order to investigate the elastic constants of the RCA samples (A_G and n_G), G_{max}, normalized with respect to the void ratio function, F(e), was plotted against the normalized confining pressure, (p'/p_A). In the study, the following void ratio function was adopted [20], which expression has been widely used for variable types of granular soils.

$$F(e) = \frac{1}{e^{1.3}} \tag{4}$$

The normalization of G_{max} with respect to the void ratio function, eliminated in a satisfactory manner the effect of sample density on G_{max}, as shown for representative samples in Fig. 10, which samples were prepared at variable initial densities. Through this procedure and a best-fit of the experimental data with a power-law type curve, the elastic constants A_G and n_G for all the samples were determined and discussed in the next section.

3.2. The effect of d_{50} on G_{max}

For all the RCA samples, the elastic constants A_G and n_G against d_{50} are plotted in Figs. 11(a) and (b), respectively. Within the scatter of the data, A_G was found not strongly dependent on the mean grain size, whereas there was observed a slight decrease of the power n_G for the coarser RCA fractions. The average value of the constant A_G within the total range of the mean grain size of the

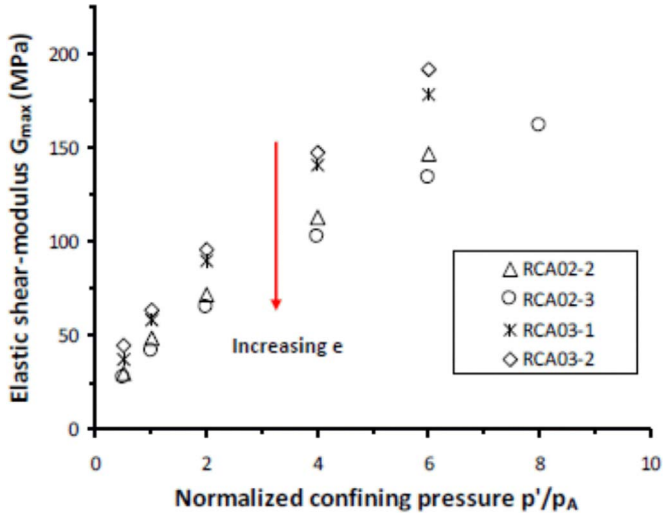

Fig. 9. Typical plots of the elastic shear-modulus against the normalized confining pressure for the fraction RCA02 (0.15–0.30 mm) and the fraction RCA03 (0.30–0.60 mm).

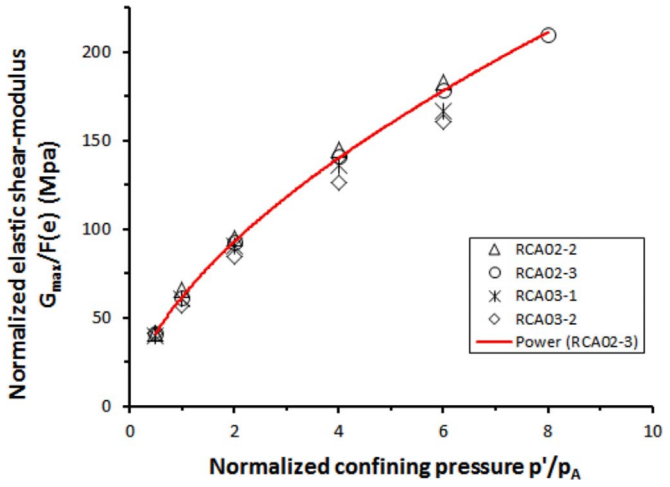

Fig. 10. Typical plots of normalized elastic shear-modulus with respect to a void ratio function against the normalized confining pressure for the fraction RCA02 (0.15–0.30 mm) and the fraction RCA03 (0.30–0.60 mm).

study, was found equal to 67.7 MPa, with a standard deviation of 7.9 MPa. n_G could be expressed as a function of d_{50} with a power-law type formula as shown in Eq. (5), in which expression d_{50} is expressed in mm.

$$n_G = 0.54 \times (d_{50})^{-0.07} \quad (5)$$

Previous research works have shown a clear tendency of decreasing n_G values for sands with more regular-shaped grains than that of sands with more irregular-shaped grains (e.g. [13,30,25]). Based on the quantification of the particle shape descriptors (Fig. 7), the RCA fractions had slightly more irregular-shaped grains with an increase of d_{50}, thus the decreasing values of the power n_G could not be the result of particle shape effects, which would give rise, otherwise, to the opposite trend, i.e. increasing n_G values for the coarser fractions. Therefore, for the RCA fractions of the study, the variation in the relative percentages of aggregate and cement mortar components with mean grain size is the possible factor that controls the sensitivity of G_{max} to pressure which was demonstrated from the SEM-EDS analysis and the variation of the ratio (Si/Ca) in Fig. 5. The finer the size of the RCA, the more pronounced the percentage of cement mortar component was

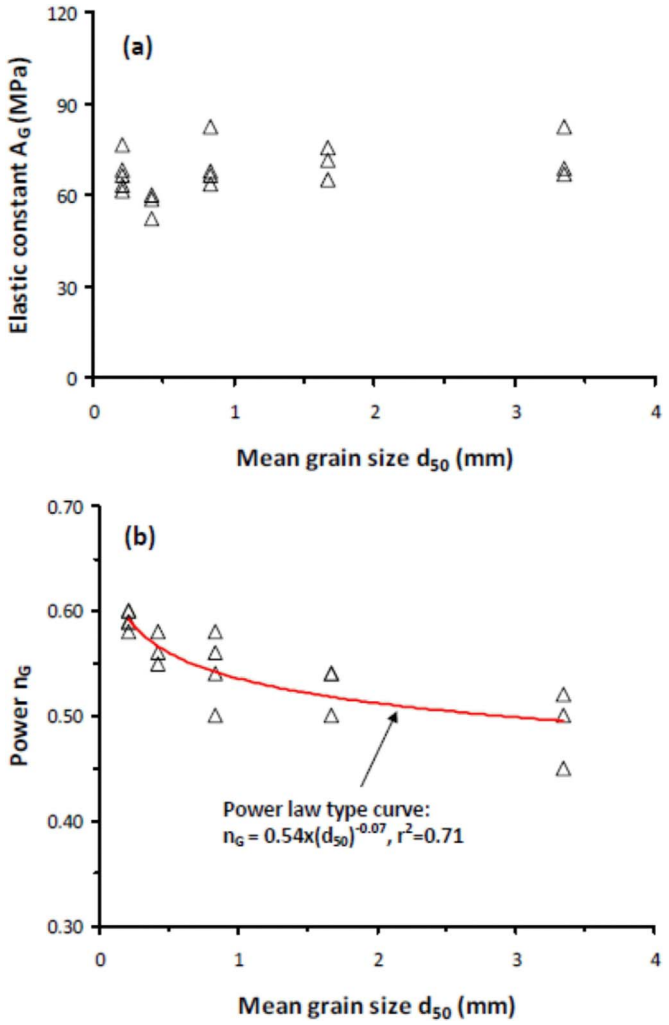

Fig. 11. The effect of the mean grain size on the elastic shear-modulus constants: (a) Elastic constant A_G against d_{50} and (b) Power n_G against d_{50}.

found which trend is aligned with the reported results in the literature [36], thus, the presence of cement mortar component seems to play an important role in the fabric changes of the samples during the increase of (p′), which fabric changes were mirrored from the greater n_G values with a decrease of the RCA fraction size.

A previous study by Cha et al. [10] demonstrated that the power n_G is linked to the compressibility of the sand which is expressed through the compressibility index (C_c) and that for more compressible sands, greater values of n_G are observed. The authors examined the compressibility of the RCA fractions through one-dimensional compression tests, but these results are not shown in the present work. However, it is noticed that there was not observed a tendency of higher compressibility of the samples for the finer fractions, thus, there could not be observed a clear relationship between the power n_G and the compressibility of the RCA fractions. This may be the result of the coupled effect of particle shape, with higher compressibility for samples with more angular grains (coarser RCA fractions), and cement mortar component which gives rise to higher compressibility for the finer fractions. Similarly, during the increase of the confining pressure (p′), the records of sample axial strain of the samples, did not demonstrate significant difference in the axial strains observed for the variable fractions. On the other hand, the grading curves of the samples were examined through a series of sieves, after the performance of the resonant column tests. For the range of confining

pressures in the study, between 25 and 800 kPa, there was not observed a significant global grain breakage that would lead to an alteration of the grading curves of the samples in comparison to the parent grading curves. Therefore, the slightly higher sensitivity of G_{max} to pressure for the finer fractions, is related, partly, to the greater cement mortar component for finer RCA fractions.

3.3. Summary of expressions proposed in the literature for the prediction of G_{max} of granular soils

In the literature, there have been proposed numerous expressions for the prediction of the elastic shear modulus of granular soils, which expressions follow the general formula of Eq. (2) with differences on the proposed void ratio functions, F(e), or the approach to normalize the confining pressure (p′). The common practice in evaluating an expression for G_{max} with respect to its predictive capacity, is to plot the estimated-predicted stiffness against the measured stiffness. Six models proposed in the literature for the prediction of G_{max} of sands and gravels are evaluated with respect to their predictive capacity for the stiffness of the RCA fractions. These six models are summarized in this section.

(a) Hardin and Richart [16] expression
Hardin and Richart [16] proposed two different expressions for the prediction of G_{max} of sands; one expression for sands of rounded grains and an other expression for sands of angular grains. The expression for sands of angular grains, which might match better to the shape of the RCA particles, is used in the study. This expression is given in Eq. (6), where (p′) is expressed in kPa and G_{max} is expressed in MPa. Hardin and Richart [16] did not apply a normalization to the confining pressure and they incorporated the effect of the shape of grains solely through the void ratio function by proposing different F(e) formulae for sands of rounded and angular grains.

$$G_{max} = 3.3 \times \left(\frac{(2.97-e)^2}{1+e}\right) \times (p')^{0.50} \tag{6}$$

(b) Senetakis et al. [30]
Senetakis et al. [30] proposed three different expressions for the prediction of G_{max} of sands; (i) an expression for a river sand with relatively regular-shaped grains (ii) an expression for a crushed rock of sand-size with irregular-shaped grains (iii) an expression for a volcanic sand composed of rhyolitic crushed rock. The expression for crushed rock, given in Eq. (7), is used in the present study. In Eq. (7), C_u is the coefficient of uniformity and G_{max} is expressed in MPa.

$$G_{max} = (-9.45 \times C_u + 57.01) \times \left(\frac{1}{e^{0.28\times C_u + 0.98}}\right) \times \left(\frac{p'}{p_A}\right)^{0.63} \tag{7}$$

Senetakis et al. [30] incorporated the effect of C_u into the constant A_G as well as the void ratio function, but they did not incorporate, quantitatively, the effect of C_u into the expression for the power n_G or, the effect of particle shape into the expressions for A_G and n_G. Note that Eq. (7) could be applicable for C_u less than six in magnitude with respect to sands of irregular-shaped grains.

(c) Senetakis and Madhusudhan [32]
Senetakis and Madhusudhan (2015) proposed an expression for the prediction of G_{max} of a crushed rock of gravel-size and irregular-shaped grains, incorporating the effect of C_u into the expression for A_G and n_G, but they used into their model a constant value for the power of the void ratio function, equal to 1.3. This expression is given in Eq. (8), where G_{max} is expressed in MPa. Note that this formula could be applicable for C_u less than 24 in magnitude.

$$G_{max} = (-3.36 \times C_u + 81.80) \times \left(\frac{1}{e^{1.3}}\right) \times \left(\frac{p'}{p_A}\right)^{0.485\times C_u^{0.13}} \tag{8}$$

(d) Yu and Richart [39]
Yu and Richart [39] proposed an expression for the prediction of G_{max} of sands based on experiments on three different types of soils. This expression is given in Eq. (9), where (p′) is expressed in kPa and G_{max} is expressed in MPa. Yu and Richart [39] did not apply a normalization to the confining pressure.

$$G_{max} = 7.0 \times \left(\frac{(2.17-e)^2}{1+e}\right) \times (p')^{0.50} \tag{9}$$

Note that Eqs. (6) and (9) are very similar but they use different constant values for A_G and slightly different constants into the void ratio function.

(e) Wichtmann and Triantafyllidis [40]
Wichtmann and Triantafyllidis [40] proposed an expression for the prediction of G_{max} of granular soils based on experiments on sands and gravels with varying the mean grain size and the coefficient of uniformity. Their expression is given in Eq. (10), where G_{max} is expressed in MPa, while Wichtmann and Triantafyllidis applied a normalization to the confining pressure (p′).

$$G_{max} = 10^{-3} \times \left(1563 + 3.13 \times C_u^{2.98}\right) \times \left(\frac{(1.94 \times exp(-0.066C_u)-e)^2}{1+e}\right) \times (p')^{0.40\times C_u^{0.18}} \times (p_A)^{1-0.40\times C_u^{0.18}} \tag{10}$$

Note that Eq. (10) incorporates the effect of C_u into the constant A_G, the power n_G as well as the void ratio function. This formula was developed on the basis of a quartz granular material of sub-angular grains.

(f) Payan et al. [25]
Payan et al. [25] proposed recently an expression for the prediction of G_{max} of sands incorporating the effect of both the coefficient of uniformity (C_u) and the shape of particles, by means of the regularity descriptor (ρ), into the prediction of the constant A_G and the power n_G. Their expression is given in Eq. (11).

$$G_{max} = \left(84.0 \times C_u^{-0.14} \times \rho^{0.68}\right) \times \left(\frac{1}{e^{1.29}}\right) \times \left(\frac{p'}{p_A}\right)^{C_u^{0.13}\times(-0.23\times\rho+0.59)} \tag{11}$$

In Eq. (11), G_{max} is expressed in MPa and the confining pressure (p′) is normalized with respect to the atmospheric pressure (p_A). Note that Payan et al. [25] proposed, based on their experiments, a very similar power for the void ratio function (equal to 1.29) with the one used in the proposed formula by Senetakis and Madhusudhan [32] (equal to 1.30). The formula by Payan et al. [25] is the first proposed expression for G_{max} of granular materials that incorporates the effects of both the grading characteristics and particle shape, quantitatively.

These six expressions for G_{max} of granular soils (Eqs. (6) – (11)), were evaluated in the present study with respect to their

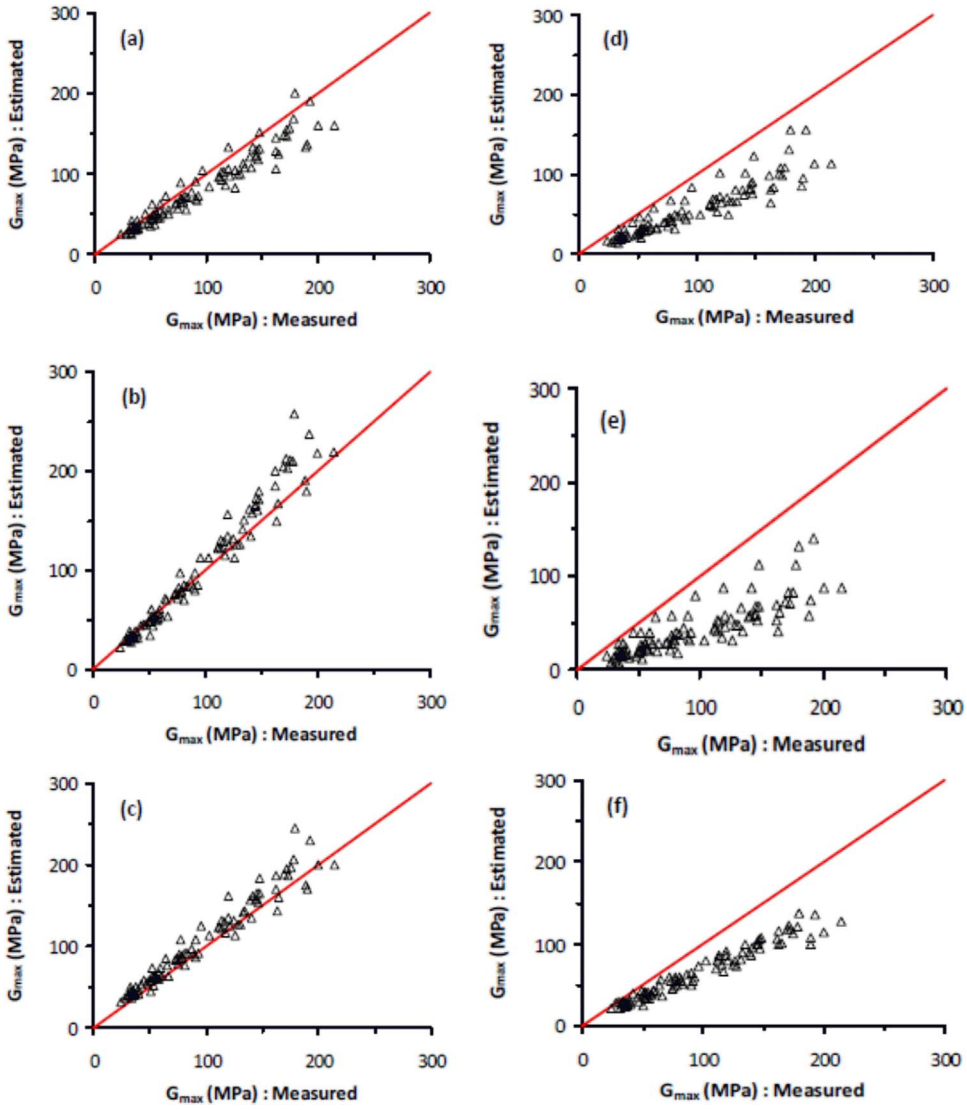

Fig. 12. Comparison of predicted against measured G_{max} using the expressions proposed by: (a) Hardin and Richart [16] (b) Senetakis et al. [30] (c) Senetakis and Madhusudhan [32] (d) Yu and Richart [39] (e) Wichtmann and Triantafyllidis (2009) (f) Payan et al. [25].

predictive capacity for the elastic stiffness of the recycled concrete aggregate fractions. This evaluation was implemented by means of predicted $G_{max,p}$ against the measured $G_{max,m}$.

3.4. The evaluation of G_{max} expressions proposed in the literature for the RCA fractions of the study by means of predicted against measured stiffness

In order to apply Eqs. (6) – (11) in the present study, the coefficient of uniformity and the mean value of the regularity that corresponded to each RCA fraction (summarized in Table 1) were used. For a given (p′), the corresponding void ratio of the samples at that level of confining pressure was used in the literature expressions. The comparison between predicted against measured G_{max} is given in Figs. 12(a) – (f).

The results in Fig. 12 showed that the expressions proposed by Hardin and Richart [16], Senetakis et al. [30] and Senetakis and Madhusudhan [32] (Eqs. (6), (7) and (8)) had a reasonably satisfactory prediction of the G_{max} of the RCA fractions, with the best prediction demonstrated by the expressions proposed by Senetakis et al. [30] and Senetakis and Madhusudhan [32]. On the other hand, the expressions of Eqs. (9), (10) and (11) systematically under-estimated the elastic stiffness of the RCA fractions. It should be mentioned that Eq. (11), proposed by Payan et al. [25], would predict a greater sensitivity of G_{max} to pressure, expressed through greater values of the power n_G, for sands with irregular-shaped grains, which is the general trend observed in previous studies as well [13,30]. For the RCA fractions of the study, it was found that the coarser fractions had slightly lower values of the mean regularity, but the results of the study showed that the power n_G decreased with an increase of d_{50}, which trend was attributed, partly, to the higher content of cement mortar component for the finer RCA fractions as demonstrated from the SEM-EDS analysis. The change of composition with the grain size led to an increase of the sensitivity of G_{max} to pressure with a decrease of d_{50}. Thus, due to the presence of aggregate and cement mortar components in the RCA fractions and their varying content with d_{50}, the expression of Eq. (11) would not provide a reliable estimation of the G_{max} for the particular demolition material.

3.5. The evaluation of G_{max} expressions proposed in the literature for the RCA fractions of the study by means of the state parameter

Payan et al. [25] showed that the predictive capacity of G_{max} models should be evaluated not only by means of predicted against measured values, but also by means of the state parameter.

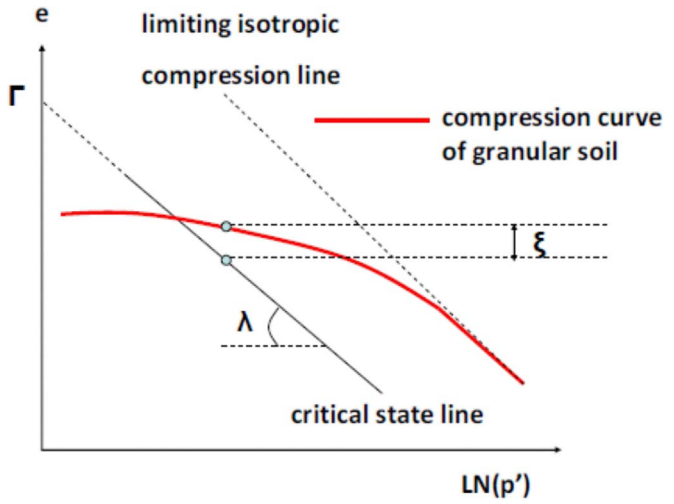

Fig. 13. The definition of the state parameter on the void ratio - pressure plane.

The state parameter (ξ) was introduced by Been and Jefferies [7]. Considering that for granular soils, the limiting isotropic (ISO) compression line is normally reached at relatively high pressures, and that the compression path curve is given in Fig. 13 in the void ratio (e) - LN(p′) plane, (ξ) is defined as the vertical distance (or difference in void ratio) between the current state of the soil, which current state is expressed from the void ratio (e) that corresponds to the compression path curve, and the critical state line (that expresses for a given p′ the critical state void ratio e_{cr}), expressed through Eq. (12).

$$\xi = e - e_{cr} \tag{12}$$

Positive values of the parameter (ξ) imply that the current void ratio is greater than the critical void ratio and that the soil is on the wet side of the critical [5]. Note that in Fig. 13, parameter (Γ) expresses the critical void ratio at p′=1 kPa (or at LN(p′)=0) and parameter (λ) expresses the slope of the critical state line in the e - LN(p′) plane. If an expression for G_{max} is truly valid for a particular soil, then in case that the ratio of the measured over the predicted elastic stiffness ($G_{max,m}/G_{max,p}$) is plotted against the state parameter (ξ), ($G_{max,m}/G_{max,p}$) should be close to unity and independent of (ξ). Payan et al. [25], showed that while some G_{max} expressions had a satisfactory performance for particular soils by means of predicted against measured values, when the ratio ($G_{max,m}/G_{max,p}$) was plotted against the state parameter, there was observed a clear trend of decreasing or increasing ($G_{max,m}/G_{max,p}$) with an increase of (ξ).

In the present study the evaluation of G_{max} expressions with respect to their predictive capacity for the recycled concrete aggregate fraction RCA04, by means of the state parameter, was also examined. Out of the six models presented in the previous section, only the models by Hardin and Richart [16], Senetakis et al. [30] and Senetakis and Madhusudhan [32] were evaluated by means of the state parameter, because these three models showed a satisfactory performance by means of predicted against measured G_{max} for the RCA fractions as shown in Fig. 12. For the fraction RCA04, monotonic triaxial tests were carried out (summarized by [17]) and the critical state parameters were found equal to Γ=2.56 and λ=0.21. In Fig. 14, the ratio ($G_{max,m}/G_{max,p}$) is plotted against the state parameter. Note that the lower values of the horizontal axis (i.e. the lower values of the state parameter ξ) corresponded to denser samples and lower confining pressures (p′), and the samples were on the dry side of the critical, and that the higher values of the horizontal axis corresponded to looser samples and higher confining pressures (p′), and the samples were on the wet side of the critical.

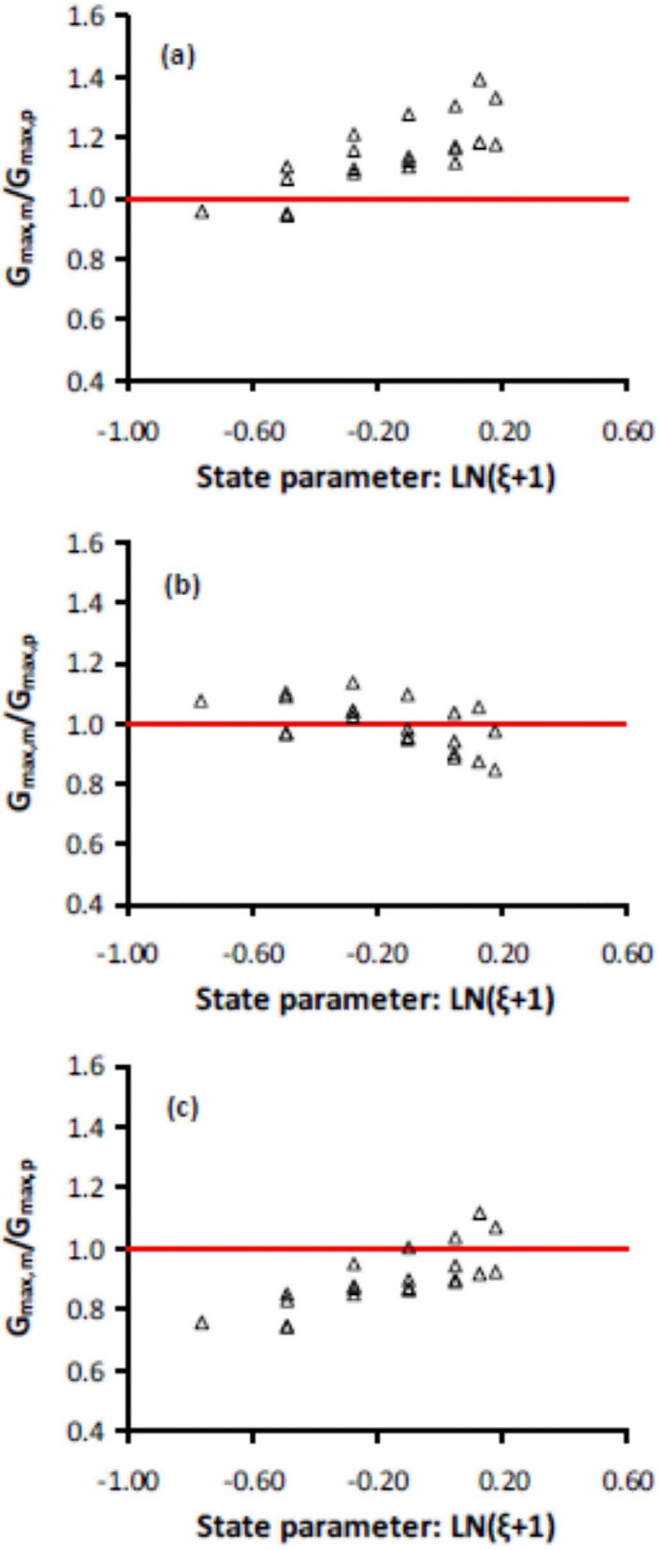

Fig. 14. Ratio of the measured over the predicted elastic shear-modulus against the parameter based on literature formulae for G_{max} prediction: (a) Hardin and Richart [16] (b) Senetakis et al. [30] (c) Senetakis and Madhusudhan [32].

In Fig. 12(a), it was shown that the G_{max} expression proposed by Hardin and Richart [16] had a satisfactory prediction of the measured stiffness of the RCA, but there was observed a slight under-estimation of the measured G_{max}. This was mirrored in the

greater than unity values of the ratio ($G_{max,m}/G_{max,p}$) shown in Fig. 14(a). This figure also showed a dependency of the ratio ($G_{max,m}/G_{max,p}$) to the state parameter. Similarly, a slight dependency of the ratio ($G_{max,m}/G_{max,p}$) to the state parameter was observed in Fig. 14(c), in which figure the G_{max} expression proposed by Senetakis and Madhusudhan [32] was used. On the other hand, the results of Fig. 14(b) showed a much better performance of the model proposed by Senetakis et al. [30] for crushed rock, with values of the ratio ($G_{max,m}/G_{max,p}$) close to unity and almost independent on the state parameter.

4. Conclusions

In the study, the effect of the mean grain size (d_{50}) on the elastic stiffness (G_{max}) of uniform fractions of a recycled concrete aggregate was examined. A set of resonant column tests in torsional mode of vibration and bender element tests using piezo-element inserts embedded in a triaxial apparatus were carried out on isotropically consolidated dry samples. The mean grain size of the samples ranged from 0.21 to 3.35 mm and the applied confining pressure ranged from 25 to 800 kPa. Denser samples were prepared with compaction in layers using vibration and looser samples were prepared with the air-pluviation method. The shape of the recycled concrete aggregate (RCA) particles was examined through visual observation in an optical microscope of a representative number of grains. Particle shape was quantified by means of three shape descriptors; the sphericity (S), the roundness (R), and the regularity (ρ). It was found the coarser fractions had slightly lower values of the regularity, thus more irregular-shaped grains than the finer fractions. SEM-EDS analysis was carried out on representative fractions of the RCA as well as on a sample composed dominantly of cement. This analysis indicated a clear increase of the ratio Silicon over Calcium for the coarser fractions, which trend indicated a decreasing content of cement for coarser RCA fractions. The dynamic test results were plotted by means of G_{max}, normalized with respect to a void ratio function F(e), against the normalized pressure (p'/p_A), where p_A is the atmospheric pressure. Through best fitting with a power-law type formula, the constant A_G and the power n_G of the (G_{max}) - (p'/p_A) relationships were evaluated. The analysis of the results showed that A_G was almost independent on d_{50}, but the power n_G decreased slightly with an increase of the mean grain size, thus the sensitivity of G_{max} to pressure was dependent on the grain size of the fraction. This trend was attributed, partly, to the increase of the cement mortar component for fractions with finer grain size as demonstrated from the SEM-EDS analysis. Six G_{max} expressions from the literature, derived on the basis of sands and gravels, were evaluated with respect to their predictive capacity on the elastic stiffness of the RCA fractions. This evaluation was implemented by means of predicted ($G_{max,p}$) against measured ($G_{max,m}$) stiffness for all the fractions, as well as by means of the ratio ($G_{max,m}/G_{max,p}$) against the state parameter (ξ) for a particular fraction. The optimum expression with respect to its predictive capacity was a model proposed in the literature for crushed rock of irregular-shaped grains.

Acknowledgments

Professor Stephen Foster (Head of School of Civil and Environmental Engineering UNSW) is acknowledged for his generous finance support in the development of the new advanced Soil Dynamics facilities of the Geotechnical Engineering Laboratory of UNSW. Mrs Songyan Yin is acknowledged for her guidance during the conduction of the SEM-EDS experiments and analysis. The anonymous reviewers are acknowledged for their constructive comments that helped us to improve the quality of the manuscript.

References

[1] Arulrajah A, Piratheepan J, Disfani MM, Bo MW. Geotechnical and geoenvironmental properties of recycled construction and demolition materials in pavement subbase applications. J Mater Civ Eng ASCE 2013;25:1077–88.
[2] Akhtaruzzaman AA, Hasnat A. Properties of concrete using crushed brick as aggregate. Concr Int 1983;5(2):58–63.
[3] ASTM. Standard Test Methods for Modulus and Damping of Soils by The Resonant Column Method: D4015-92. Annual Book of ASTM Standards. USA: ASTM International; 1992.
[4] ASTM. Standard Test Methods for Specific Gravity of Soil Solids by Water Pycnometer: D854-022. Annual Book of ASTM Standards. USA: ASTM International; 2002.
[5] Atkinson J. An Introduction to The Mechanics of Soils and Foundations. McGraw-Hill International Series in Civil Engineering; 1993.
[6] Banasiak L, Indraratna B, Regmi G, Golab A, Lugg G. Characterization and assessment of recycled concrete aggregate used in a permeable reactive barrier for the treatment of acidic groundwater. Geomech Geoengin 2013;8(3):155–66.
[7] Been K, Jefferies MG. A state parameter for sands. Geotechnique 1985;35(2):99–112.
[8] Bhuiyan MZI, Ali FHj, Salman FA. Applications of recycled concrete aggregates as alternative granular infills in hollow segmental block systems. Soils Found 2015;55(2):296–303.
[9] Cascante G, Santamarina C. Interparticle contact behavior and wave propagation. J Geotech Geoenviron Eng ASCE 1996;122:831–9.
[10] Cha MC, Santamarina JC, Kim H-S, Cho G-C. Small-strain stiffness, shear-wave velocity, and soil compressibility. J Geotech Geoenviron Eng ASCE 2014;140:06014011.
[11] Chang N-Y, Ko H-Y. Effect of grain size distribution on dynamicproperties and liquefaction potential of granular soils Research Report R82-103. USA: University of Colorado at Denver,; 1982.
[12] Chini AR, Kuo SS, Armaghani JM, Duxbury JP. Test of recycled concrete aggregate in accelerated test track. J Transp Eng 2001;127(6):486–92.
[13] Cho G-C, Dodds J, Santamarina C. Particle shape on packing density, stiffness, and strength. J Geotech Geoenviron Eng ASCE, 132; 2006. p. 591–602.
[14] Edil T, Luh G. Dynamic modulus and damping relationships for sands. In: Proceedings of the geotechnical division speciality conference on earthquake engineering and soil dynamics. Pasadena, CA, USA: ASCE; 1, 1978. p. 394–09.
[15] Gu X, Yang J, Huang M, Gao G. Bender element tests in dry and saturated sand: Signal interpretation and result comparison. Soils Found 2015;55(5):951–62.
[16] Hardin B, Richart F. Elastic wave velocities in granular soils. J Soil Mech Found ASCE 1963;89(SM1):33–65.
[17] He H, Senetakis K. A study of wave velocities and Poisson ratio of recycled concrete aggregate. Soils Found 2016, http://dx.doi.org/10.1016/j.sandf.2016.07.002.
[18] Ishihara K. Soil behaviour in earthquake geotechnics. Oxford Science Publications; 1996.
[19] Iwasaki T, Tatsuoka F. Effects of grain size and grading on dynamic shear moduli of sands. Soils Found 1977;17(3):19–35.
[20] Jamiolkowski M, Leroueil S and Lo Priesti D. Design parameters from theory to practice. In: Proceedings of the International Conference on Geotechnical Engineering for Coastal Development: Geo-Coast, Coastal Development Institute of Technology. Yokohama, Japan; 1991. p. 877–17.
[21] Jovicic V, Coop MR, Simic M. Objective criteria for determining G_{max} from bender element tests. Geotechnique 1996;46(2):357–62.
[22] Knight RD, Klassen RA, Hunt P. Mineralogy of fine-grained sediment by energy-dispersive spectrometry (EDS) image analysis - a methodology. Environ Geol 2002;42:32–40.
[23] Krumbein W, Sloss L. Stratigraphy and Sedimentation.Freeman and Company. San Francisco: W.H,; 1963.
[24] Menq F-Y. Dynamic Properties of Sandy and Gravelly Soils (Ph.D. Dissertation). USA: University of Texas at Austin,; 2003.
[25] Payan M, Khoshghalb A, Senetakis K, Khalili N. Effect of particle shape and validity of G_{max} models for sand: A critical review and a new expression. Comput Geotech 2016;72:28–41.
[26] Poon CS, Chan D. Feasible use of recycled concrete aggregates and crushed clay brick as unbound road sub-base. Constr Build Mater 2006;20:578–85.
[27] Richart FE, Hall JR, Woods RD. Vibrations of Soils and Foundations.Englewood Cliffs: Prentice Hall,; 1970. p. 414.
[28] Santamarina C, Cascante G. Effect of surface roughness on wave propagation parameters. Geotechnique 1998;48(1):129–36.
[29] Santamarina C, Klein K, Fam M. Soils and WAVES.New York: John Wiley and Sons,; 2001.
[30] Senetakis K, Anastasiadis A, Pitilakis K. The small-strain shear modulus and damping ratio of quartz and volcanic sands. Geotech Test J 2012;35(6). http://dx.doi.org/10.1520/GTJ20120073.

[31] Senetakis K, Anastasiadis A, Pitilakis K, Coop M. The dynamics of a pumice granular soil in dry state under isotropic resonant column testing. Soil Dyn Earthq Eng 2013;45:70–9.
[32] Senetakis K, Madhusudhan BN. Dynamics of potential fill-backfill material at very small strains. Soils Found 2015;55(5):1196–210.
[33] Senetakis K, Madhusudhan BN, Anastasiadis A. On the wave propagation attenuation and threshold strains of fully saturated soils with intra-particle voids. J Mater Civ Eng ASCE 2015 10.1061/(ASCE)MT.1943–5533.0001367, 04015108.
[34] Sivakumar V, McKinley JD, Ferguson D. Reuse of construction waste: performance under repeated loading. Proc Inst Civ Eng: Geotech Eng 2004;157 (2):91–6.
[35] Shirley D, Anderson A. In situ measurement of marine sediment acoustical properties during coring in deep water. IEEE Trans Geosci Electron 1975;GE-13:163–9.
[36] Tam VWY, Tam CM. "Crushed aggregate production from centralized combined and individual waste sources in Hong Kong. Constr Build Mater 2007;21 (4):879–86.
[37] Tatsuoka F, Tomita YI, Iguchi Y, Hirakawa D. Strength and stiffness of compacted crushed concrete aggregate. Soils Found 2013;53(6):835–52.
[38] Yang J, Gu XQ. Shear stiffness of granular material at small strains: does it depend on grain size? Geotechnique 2013;63(2):165–79.
[39] Yu P, Richart F. Stress ratio effects on shear modulus of dry sands. J Geotech Eng ASCE 1984;110(3):331–45.
[40] Wichtmann T, Triantafyllidis Th. Influence of the grain-size distribution curve of quartz sand on the small strain shear modulus G_{max}. J Geotech Geoenviron Eng ASCE 2009;135(10):1404–18.